



Constraining the ship contribution to the aerosol of the central Mediterranean

Silvia Becagli¹, Fabrizio Anello², Carlo Bommarito², Federico Cassola^{3,4}, Giulia Calzolai⁵, Tatiana Di Iorio⁶, Alcide di Sarra⁶, José-Luis Gómez-Amo^{6,7}, Franco Lucarelli⁵, Miriam Marconi¹, Daniela Meloni⁶, Francesco Monteleone², Silvia Nava⁵, Giandomenico Pace⁶, Mirko Severi¹, Damiano Massimiliano Sferlazzo⁸, Rita Traversi¹, and Roberto Udisti^{1,9}

¹Department of Chemistry, University of Florence, Sesto Fiorentino, 50019 Florence, Italy

²ENEA, Laboratory for Observations and Analyses of Earth and Climate, 90141 Palermo, Italy

³Department of Physics & INFN, University of Genoa, 16146 Genoa, Italy

⁴ARPAL-Unità Operativa CFMI-PC, 16129 Genova, Italy

⁵Department of Physics, University of Florence & INFN-Firenze, Sesto Fiorentino, 50019 Florence, Italy

⁶ENEA, Laboratory for Observations and Analyses of Earth and Climate, 00123 Rome, Italy

⁷Department of Earth Physics and Thermodynamics, University of Valencia, Valencia, Spain

⁸ENEA, Laboratory for Observations and Analyses of Earth and Climate, 92010 Lampedusa, Italy

⁹ISAC CNR, Via Gobetti 101, 40129, Bologna, Italy

Correspondence to: Silvia Becagli (silvia.becagli@unifi.it)

Received: 8 June 2016 – Discussion started: 1 July 2016

Revised: 23 November 2016 – Accepted: 19 January 2017 – Published: 10 February 2017

Abstract. Particulate matter with aerodynamic diameters lower than 10 μm , (PM_{10}) aerosol samples were collected during summer 2013 within the framework of the Chemistry and Aerosol Mediterranean Experiment (ChArMEx) at two sites located north (Capo Granitola) and south (Lampedusa Island), respectively, of the main Mediterranean shipping route in the Strait of Sicily.

The PM_{10} samples were collected with 12 h time resolutions at both sites. Selected metals, main anions, cations and elemental and organic carbon were determined.

The evolution of soluble V and Ni concentrations (typical markers of heavy fuel oil combustion) was related to meteorology and ship traffic intensity in the Strait of Sicily, using a high-resolution regional model for calculation of back trajectories. Elevated concentration of V and Ni at Capo Granitola and Lampedusa are found to correspond with air masses from the Strait of Sicily and coincidences between trajectories and positions of large ships; the vertical structure of the planetary boundary layer also appears to play a role, with high V values associated with strong inversions and a stable boundary layer. The V concentration was generally lower at

Lampedusa than at Capo Granitola V, where it reached a peak value of 40 ng m^{-3} .

Concentrations of rare earth elements (REEs), La and Ce in particular, were used to identify possible contributions from refineries, whose emissions are also characterized by elevated V and Ni amounts; refinery emissions are expected to display high La/Ce and La/V ratios due to the use of La in the fluid catalytic converter systems. In general, low La/Ce and La/V ratios were observed in the PM samples. The combination of the analyses based on chemical markers, air mass trajectories and ship routes allows us to unambiguously identify the large role of the ship source in the Strait of Sicily.

Based on the sampled aerosols, ratios of the main aerosol species arising from ship emission with respect to V were estimated with the aim of deriving a lower limit for the total ship contribution to PM_{10} . The estimated minimum ship emission contributions to PM_{10} were 2.0 $\mu\text{g m}^{-3}$ at Lampedusa and 3.0 $\mu\text{g m}^{-3}$ at Capo Granitola, corresponding with 11 and 8.6 % of PM_{10} , respectively.

1 Introduction

Ship emissions may significantly affect atmospheric concentrations of several important pollutants, especially in maritime and coastal areas (e.g. Endresen et al., 2003). Main emitted compounds are carbon dioxide (CO₂), nitrogen oxides (NO_x), sulfur dioxide (SO₂), carbon monoxide (CO), hydrocarbons and primary as well as secondary particles. Thus, ship emissions impact the greenhouse gas budget, (Stern, 2007), acid rain – through NO_x and SO₂ oxidation products (Derwent et al., 2005), human health – through CO, hydrocarbons, particles (Lloyd's Register Engineering Services, 1995; Corbett et al., 2007) and solar radiation budget through aerosol direct and indirect effects such as black carbon and sulfur containing particles (Devasthale et al., 2006; Lauer et al., 2007; Coakley Jr. and Walsh, 2002).

Heavy oil fuels used by ships contain varying transition metals. The aerosol emitted by ship engines is formed at high temperatures (> 800 °C) from V, Ni and Fe compounds (Sippula et al., 2009). The thermodynamics predict that the metals in these particles are mainly present as oxides. Sulfuric acid is found to form a liquid layer on the metal oxide ultra-fine particles, leading to the metal partial dissolution, probably increasing the toxicity of the particles when inhaled.

In spite of the large amount of gas and particulate emitted by ships, maritime transport is relatively clean if calculated per kilogram of transported good. However, maritime transport has been increasing with respect to air and road transport (Micco and Pérez, 2001; Grewal and Haugstetter, 2007). In addition, emissions from other transport sectors are decreasing due to the implementation of advanced emission reduction technologies, and the relative impact of shipping emissions is increasing.

Regulations aiming at reducing emissions based on restrictions on the fuel sulfur content (sulfur emission control areas, or SECAs) have been implemented in several regions. Although the legislation is focussed on sulfur emissions, the overall health and environmental effects depend in a complex way on the physical and chemical properties of the emissions (WHO, 2013). Several studies have been carried out to determine the detailed chemical composition of shipping emissions (Agrawal et al., 2008a, b; Moldanová et al., 2009; Murphy et al., 2009; Lyyränen et al., 1999; Cooper, 2003; Sippula et al., 2014); however, the ships emissions are still poorly characterized with respect to on-road vehicles.

A large variety of anthropic sources (refineries, power plants intense ship traffic, etc.) and natural emissions make the Mediterranean region one of the most polluted in the world (e.g. Kouvarakis et al., 2000; Marmer and Langmann, 2005). The multiplicity of Mediterranean sources (some of which with the same markers of ship aerosol) makes the quantification of ship contribution to the total aerosol amount difficult (e.g. Becagli et al., 2012).

The contribution of ships and harbour emissions to local air quality, with specific focus on atmospheric aerosol, has

been investigated using models (Trozzi et al., 1995; Gariazzo et al., 2007; Eyring et al., 2005; Marmer et al., 2009), experimental analyses at high temporal resolution (Ault et al., 2010; Contini et al., 2011; Jonsson et al., 2011; Diesch et al., 2013; Donateo et al., 2014), receptor models based on the identification of chemical tracers associated with ship emissions (Viana et al., 2009; Pandolfi et al., 2011; Cesari et al., 2014) and integrated approaches with receptor and chemical transport models (Bove et al., 2014). Few studies exist in open sea (Becagli et al., 2012; Schembari et al., 2014; Bove et al., 2016).

In this context, studies performed at Mediterranean sites where it is possible to distinguish ship emission from other sources of heavy fuel oil combustion, are important to investigate the current impact of the ship emissions on primary and secondary aerosols. This study contributes to the identification and characterization of the emissions from ships and the impact on the aerosol distribution in the central Mediterranean. The experiment was set up with the aim of unambiguously recognizing the ship source by a combination of methods.

2 Measurements and methods

In a previous study (Becagli et al., 2012), we used measurements of PM₁₀ concentration and chemical composition carried out at Lampedusa to investigate the role of ship emissions in the central Mediterranean. Vanadium and Nickel were used as tracers of heavy fuel combustion together with trajectory analyses to assess the role of ship traffic. The ship source, however, could not be unequivocally separated from possible influences from refineries and power plants, which use similar fuels. In summer 2013 we addressed the same topic by implementing a specific strategy to target the aerosols due to ship emissions. PM₁₀ samples were collected in parallel at Lampedusa (LMP) and at Capo Granitola (CGR) respectively, i.e. south and north of the main shipping route through the Mediterranean, with the aim of isolating the ship source. The chemical analyses of the collected samples were complemented with measurements of REEs, trajectories and planetary boundary layer information from a high resolution regional model and actual observations of ship traffic. The combination of these approaches allows the unambiguous identification of the ship source and permits the constraint of its contribution to PM₁₀ in the central Mediterranean. The PM₁₀ samples were collected in summer 2013 as a contribution to the Chemistry and Aerosol Mediterranean Experiment (ChArMEx; <http://charmex.lscse.ispl.fr>). Lampedusa is one of the supersites of the ChArMEx experiment; a list of the instruments deployed during the special observing period (1a) of ChArMEx, of the measurement strategy, meteorological conditions and main observations is given by Mallet et al., (2016).

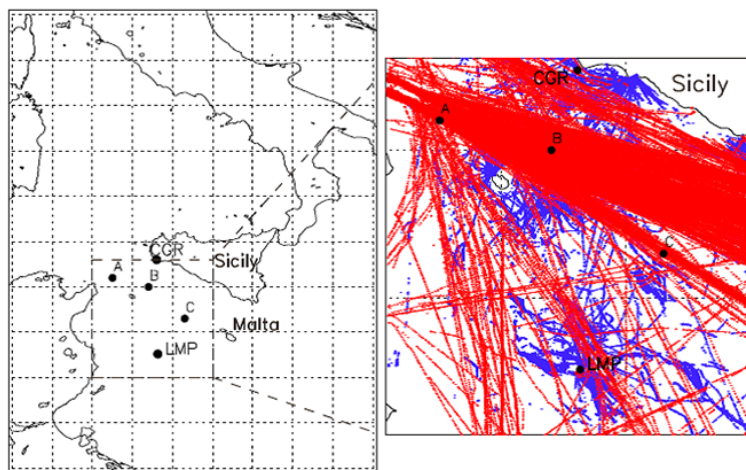


Figure 1. Map of the study area with the sites of Lampedusa (LMP) and Capo Granitola (CGR) are displayed in the left panel. A–C indicate the three sites selected to study the stability of the boundary layer in the Strait of Sicily (see Sect. 3.2.2). The ship routes in the study area during the first 10 days of June 2013 are displayed in the right panel. Red and blue dots show the routes of merchant and fishing vessels, respectively.

2.1 Aerosol sampling and chemical analyses

PM₁₀ was sampled at two sites: at the station for climate Observations, maintained by ENEA (the Italian Agency for New Technologies, Energy, and Sustainable Economic Development) on the island of Lampedusa (35.5° N, 12.6° E), and at the Italian CNR (National Research Council) Research Centre at Capo Granitola (36.6° N, 12.6° E).

Lampedusa is a small island in the Central Mediterranean sea, more than 100 km far from the nearest Tunisian coast. At the station for climate Observations, which is located on a plateau 45 m a.s.l on the northeastern coast of Lampedusa, continuous observations of aerosol properties (di Sarra et al., 2011, 2015; Becagli et al., 2013; Marconi et al., 2014; Calzolari et al., 2015; Sellitto et al., 2017), aerosol radiative effects (e.g. Casasanta et al., 2011; di Sarra et al., 2011; Meloni et al., 2015) and other climatic parameters are carried out. Figure 1 shows the map of the central Mediterranean with the measurement stations.

PM₁₀ is routinely sampled on a daily basis at LMP (Becagli et al., 2013; Marconi et al., 2014; Calzolari et al., 2015) by using a low-volume dual-channel sequential sampler (HYDRA FAI Instruments) equipped with two PM₁₀ sampling heads, operating in accord with UNI EN12341. For the intensive ChArMEx campaign, samples were collected at 12 h resolution (08:00–20:00 and 20:00–08:00 LT–local time) from 1 June to 3 August 2013.

The two channels operated in parallel and were loaded with different types of filters: the first one with 47 mm diameter, 2 μm-nominal porosity Teflon filters, and the second one with 47 mm pre-fired, 2 μm-nominal porosity quartz filters. Ion chromatographic analysis of soluble ions, atomic emission spectroscopy for soluble metals and proton-induced

X-ray emission (PIXE) for the total (soluble + insoluble) elemental composition were carried out on the Teflon filters. Elemental carbon (EC) and organic carbon (OC) were measured by analysing the quartz filters.

The sampling site at CGR is located at Torretta Granitola, a Research Center of the Italian National Research Council, in southwestern Sicily (12 km from Mazara del Vallo). The sampler was installed on the roof of one of the research centre buildings at about 20 m a.s.l., directly on the coastline, facing the Strait of Sicily.

At CGR PM₁₀ samples were collected at 12 h resolution (08:00–20:00 and 20:00–08:00 LT) with a TECORA Skypost sequential sampler on 47 mm pre-fired 2 μm-nominal porosity quartz filters, which were used to determine ions, metals, EC and OC on different fractions of the filter. Due to technical problems, some daytime (08:00–20:00 LT) samplings were lost at CGR.

The PM₁₀ mass was determined by weighting the filters before and after sampling with an analytical balance in controlled conditions of temperature (20 ± 1 °C) and relative humidity (50 ± 5 %). The estimated error on PM₁₀ mass is around 1 % at 30 μg m⁻³ in the applied sampling conditions.

A quarter of each Teflon filter from LMP and a 1.5 cm² punch of the quartz filter from CGR were analysed by Ion Chromatography (IC) in the analytical conditions described in Marconi et al., (2014). The estimated uncertainty for IC measurements is 5 % for all the considered ions.

Blank values were negligible with respect to the concentration in the samples for Teflon filters. Blank values for quartz filters were negligible for most of the analysed species. For some species characterized by high blank values, always lower than the 25th percentile value, they were subtracted from the measured concentrations.

Table 1. Sampling strategy and chemical measurements carried out on each filter for the two sites: Lampedusa (LMP) and Capo Granitola (CGR). The sampling time interval is at local time (LT).

Sampling site	Filter	Sampling interval (LT)	Measurements
LMP	Teflon	08:00–20:00 (daytime sample) 20:00–08:00 (nighttime sample)	– PM ₁₀ ; – ions by IC (1/4 of the filter); – metals in HNO ₃ pH 1.5 room temperature extract by ICP-AES (1/4 of the filter); – metals in HNO ₃ -H ₂ O ₂ in microwave oven extract by ICP-AES (1/2 filter)
	Quartz	08:00–20:00 (daytime sample) 20:00–08:00 (nighttime sample)	– EC / OC by thermo-optical analyser (1.5 cm × 1 cm punch)
CGR	Quartz	08:00–20:00 (daytime sample) 20:00–08:00 (nighttime sample)	– PM ₁₀ ; – ions by IC (1.5 cm × 1 cm punch); – metals in HNO ₃ pH 1.5 room temperature extract by ICP-AES (1.5 cm × 1 cm punch); – metals in HNO ₃ -H ₂ O ₂ in microwave oven extract by ICP-AES (1.5 cm × 1 cm punch) – EC / OC by thermo-optical analyser (1.5 cm × 1 cm punch)

Another quarter of the Teflon filter from LMP and another 1.5 cm² punch of the quartz filter from CGR were extracted in an ultrasonic bath for 15 min with MilliQ water acidified at pH 1.5–2 with ultra pure HNO₃ obtained by sub-boiling distillation. This extract was used for the metal's soluble part determination by means of an Inductively Coupled Plasma Atomic Emission Spectrometer (ICP-AES, Varian 720-ES) equipped with an ultrasonic nebulizer (U5000 AT+, Cetac Technologies Inc.). The pH chosen value is the lowest found in rainwater (Li and Aneja, 1992) and leads to the determination of the metals fraction available to biological organisms and, for some metals (e.g. V and Ni), related to the anthropic source (Becagli et al., 2012).

The remaining half Teflon filter from Lampedusa, another punch of the quartz filter from CGR, was used for the determination of metals by ICP-AES through the solubilisation procedure reported in the EU EN14902 (2005) rule, by concentrating sub-boiling distilled HNO₃ and 30 % ultra pure H₂O₂ in a microwave oven at 220 °C for 25 min (P = 55 bar). This solubilisation procedure is not able to completely dissolve the silicate species. However, this procedure allows to the recovery at least 70 % of the same elements measured by a proton induced X-ray emission technique also for elements with dominant crustal source (unpublished data) due to the low crustal aerosol load in these sampling periods (e.g. Mailler et al., 2016). La and Ce presented very low concen-

trations in the collected aerosol samples. Thus, particular attention was devoted to the minimization of the La and Ce detection limit. In the used sampling and analytical conditions of LMP samples the detection limits for La and Ce are 0.02 and 0.08 ng m⁻³, respectively, and are about 4 times higher for the CGR samples, due to the smaller filter portion used for the analysis. The OC and EC measurements were carried out on a 1.5 cm² punch of the quartz filters from Lampedusa and Capo Granitola by means of a Sunset thermo-optical transmittance analyser, following the NIOSH protocol (Wu et al., 2016).

The overall aerosol sampling and analytical strategy for the two sites are reported in Table 1.

2.2 Atmospheric model and trajectory calculations

Numerical simulations with a non-hydrostatic mesoscale atmospheric model were used to characterize the meteorological conditions in the Strait of Sicily during the campaign and to support the interpretation of the experimental results. The Weather Research and Forecasting (WRF) model (Skamarock et al., 2008) outputs, provided by the Department of Physics of the University of Genoa, Italy, were used, covering the entire Mediterranean with a grid spacing of 10 km and hourly temporal resolution. Initial and boundary conditions to drive WRF simulations were obtained from the

Global Forecast System operational global model (Environmental Modeling Center, 2003) outputs (0.5×0.5 squared degrees). Some recent applications of the modelling chain are described in Mentaschi et al., (2015) and Cassola et al., (2016), where full details on the model configuration can also be found.

In particular, the WRF 3-D hourly meteorological fields were used to calculate backward trajectories with the NOAA HYbrid Single-Particle Lagrangian Integrated Trajectory Model (HYSPLIT; Stein et al., 2015). The trajectories were used to assess the origin of the air masses impacting the monitoring sites and to support the source attribution suggested by the analysis of specific markers (see Sect. 3.2.2). The use of a high-resolution regional atmospheric model for trajectory calculations allows for a better representation of boundary layer properties and mesoscale phenomena such as land and sea breezes, which can have a relevant impact especially in complex topography coastal sites like CGR.

Also, the high temporal resolution of meteorological data (hourly instead of three- or six-hourly products typically available from global models) permits a better description of diurnal cycles and a more accurate trajectory computation without time interpolation between subsequent atmospheric fields (Solomos et al., 2015).

Specifically, 48 h-long back trajectories arriving at LMP and CGR were computed from a reference height of 10 m above the ground level, starting every six hours for the whole period of the campaign, from 10 June to 31 July 2013.

2.3 Ships/marine traffic

Position and main characteristics of the ships travelling in the central Mediterranean were derived from the Marine-Traffic database (<http://www.marinetraffic.com/>), which provides data with a high temporal resolution (about 3–5 min) by means of the Automatic Identification System (AIS).

Three classes of ships defined by the AIS classification were considered: all the ships, the merchant ships (i.e. cargo and tanker) and the fishing vessels. Merchant and fishing vessels are the most frequent ships in the Strait of Sicily; merchant ships are expected to produce the highest impact due to their higher emissions (http://ec.europa.eu/environment/archives/air/pdf/chapter2_ship_emissions.pdf).

3 Results

3.1 PM₁₀ chemical composition at the two sites

The sea salt aerosol (SSA) component of PM₁₀ was estimated as the sum of Na⁺, Mg²⁺, Ca²⁺, K⁺, sulfate and chloride sea salt (ss) fractions. Details on the calculation of sea salt Na⁺ and Ca²⁺, and non-sea salt (nss) fractions are reported in Marconi et al., (2014). The Mg²⁺, Ca²⁺, K⁺ and sulphate sea salt fractions were calculated from sea salt Na⁺ (ssNa⁺) by using the ratio of each component to Na⁺ in

bulk sea water: Mg²⁺/Na⁺ = 0.129, Ca²⁺/Na⁺ = 0.038, K⁺/Na⁺ = 0.036, SO₄²⁻/Na⁺ = 0.253 (Bowen, 1979). Chloride undergoes depletion processes during the aging of sea spray, mainly due to exchange reactions with anthropogenic H₂SO₄ and HNO₃, leading to the re-emission of gaseous HCl in the atmosphere. Thus, for chloride we use the measured chloride concentration instead of the one calculated from ssNa⁺. Thus,

$$\text{SSA} = 1.46 \cdot [\text{ssNa}^+] + [\text{Cl}^-].$$

The crustal component is calculated from Al, which represents 8.2 % of the upper continental crust, UCC (Henderson and Henderson, 2009). A previous study using an extensive data set at Lampedusa showed that the crustal content determined from the total Al was in very good agreement with calculations made from the sum of the metal oxides (Marconi et al., 2014). However, in this study we use measurements of the soluble Al concentration obtained by ICP-AES on the solution obtained with H₂O₂ and HNO₃ in a microwave oven instead of the total Al content. Therefore, in this work we underestimate the crustal contribution by about 30 % (unpublished results). However, it must be emphasized that the crustal aerosol contribution has been very low throughout the measurement campaign.

Figure 2 shows the time series of the main PM₁₀ components at LMP and CGR. An intense mistral event occurred from 22 June to 1 July. Mistral events are characterized by strong winds from the northwesterly sector and often by subsiding air masses originating from the free troposphere (Jiang et al., 2003). Thus, elevated values of SSA and low concentrations of other compounds are generally found during mistral at Lampedusa.

Average concentrations of PM₁₀ and of the different aerosol components for the whole measurement campaign and for the non-mistral conditions are reported in Table 2. The averages were calculated over a homogeneous data set, i.e. when measurements are available at both sites.

The largest PM₁₀ values were associated with elevated SSA during the mistral event at both sites. PM₁₀ is about two times larger at Capo Granitola than at Lampedusa. The PM₁₀ measured during the campaign at Lampedusa was significantly lower than its long-term average ($31.5 \mu\text{g m}^{-3}$; Marconi et al., 2014). No Saharan dust transport events occurred at low altitude in this period (e.g. Mailler et al., 2016), and the crustal aerosol contribution remained very low and almost constant at both sites (average $< 1 \mu\text{g m}^{-3}$ at LMP and around $3 \mu\text{g m}^{-3}$ at CGR, corresponding to 4.6 and 8.2 % of the PM₁₀ at LMP and CGR respectively).

SSA accounted for about 26 and 24 % of PM₁₀ at LMP and CGR, respectively. The SSA contribution was about 14 % of PM₁₀ at LMP and 8 % at CGR during the periods not influenced by the mistral. Non-sea salt SO₄²⁻ was the most abundant among the secondary inorganic species.

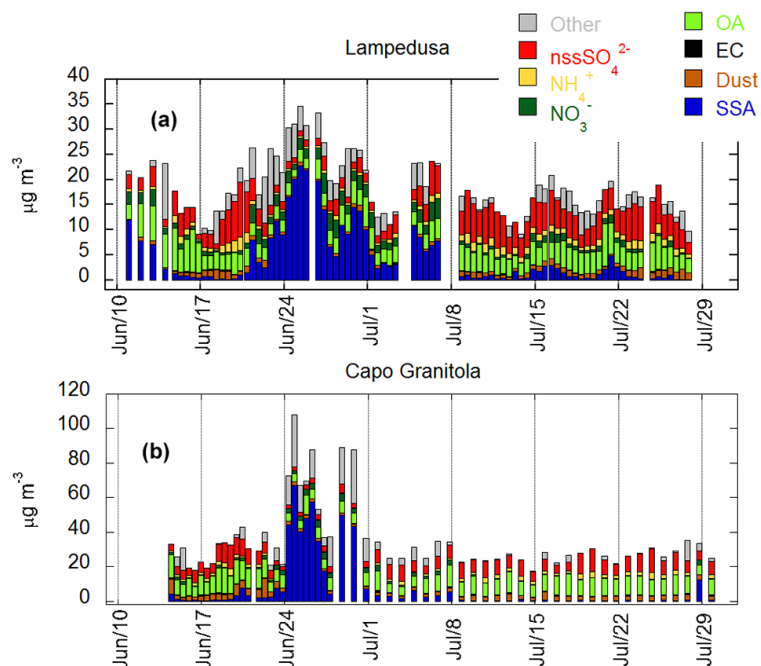


Figure 2. Time series of the main aerosol components at LMP (a) and CGR (b). Note the different vertical scales of the graphs. OA, EC, and SSA stand for organic aerosol, elemental carbon and sea salt aerosol, respectively.

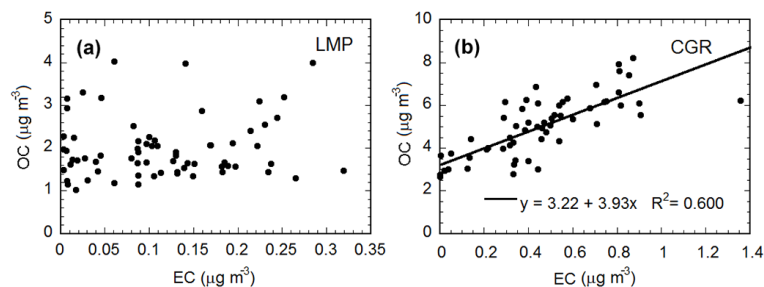


Figure 3. Scatter plot of OC vs. EC at LMP (a) and CGR (b). Note the different vertical scales.

Nitrate concentrations, although relatively high at both sites, are in agreement with the long term measurements performed at Lampedusa (e.g. Calzolari et al., 2015) and with data from other remote sites in the western (Mallorca; e.g. Simo et al., 1991) and eastern Mediterranean (Finokalia; e.g. Mihalopoulos et al., 1997).

Organic aerosol (OA) was the most abundant component at CGR, where its mean concentration was $> 9 \mu\text{g m}^{-3}$ and represented 35 % of PM_{10} in the days not characterized by the mistral.

Elemental carbon and organic carbon show higher values at CGR than LMP. At CGR, moderate and elevated values of OC and EC appear correlated ($R^2 = 0.60$; $n = 59$; Fig. 3b), suggesting a strong influence of carbon species from primary sources, characterized by the simultaneous EC and OC emission. The influence from primary sources is apparent at $\text{EC} > 0.4 \mu\text{g m}^{-3}$. At LMP, on the contrary, OC was not cor-

related with EC (Fig. 3a), indicating a strong impact of OC secondary and/or natural sources. This confirms that Lampedusa may be considered a background site in the central Mediterranean (see e.g. Artuso et al., 2009; Henne et al., 2010), and the observations there may be taken as representative for a relatively wide open sea region.

Thus, we used a conversion factor of 1.8 (typical for urban background sites, Turpin and Lim, 2001) at CGR, and of 2.1 (typical for remote sites characterized by the high impact of secondary sources, Turpin and Lim, 2001) at LMP to estimate the total organic aerosol amount from the OC measured values. Once we estimated OA with this method, the sum of the various species accounted for more than 85 % of the measured mass at both sites. The unreconstructed mass could be due to an underestimation of OA from OC, or to the presence of bound water not removed by the desiccation procedure at 50 % relative humidity (Tsyro, 2005; Canepari et al., 2013).

Table 2. Mean and standard deviation of PM₁₀ load and composition, and percentage with respect to PM₁₀ (in brackets) at Lampedusa and Capo Granitola. Mean, standard deviation and percentage are calculated on homogeneous data sets for both sites, considering all the common sampling (“all data” columns) and excluding the mistral events (“mistral excluded” columns).

	Lampedusa		Capo Granitola	
	All data	Mistral excluded	All data	Mistral excluded
PM ₁₀ (μg m ⁻³)	18.0 ± 6.6	16.3 ± 5.2	34.1 ± 18.9	27.2 ± 6.5
Sea Salt Aerosol (μg m ⁻³)	4.63 ± 6.30 (25.7 %)	2.33 ± 3.21 (14.3 %)	8.14 ± 15.50 (23.9 %)	2.12 ± 6.51 (7.8 %)
Crustal Aerosol (μg m ⁻³)	0.82 ± 0.44 (4.6 %)	0.90 ± 0.43 (5.5 %)	2.80 ± 1.7 (8.2 %)	3.02 ± 1.75 (11.1 %)
nssSO ₄ ²⁻ (μg m ⁻³)	3.95 ± 2.28 (21.9 %)	4.40 ± 2.22 (27.0 %)	6.78 ± 3.08 (19.9 %)	7.53 ± 2.78 (27.7 %)
NH ₄ ⁺ (μg m ⁻³)	0.98 ± 0.56 (5.5 %)	1.09 ± 0.55 (6.7 %)	1.48 ± 0.94 (4.3 %)	1.66 ± 0.87 (6.1 %)
NO ₃ ⁻ (μg m ⁻³)	1.25 ± 1.00 (7.0 %)	1.02 ± 0.02 (6.2 %)	1.35 ± 1.11 (4.0 %)	1.01 ± 0.82 (3.7 %)
Organic aerosol (μg m ⁻³)	3.86 ± 1.56 (21.4 %)	4.04 ± 1.59 (24.8 %)	9.02 ± 2.52 (26.5 %)	9.53 ± 2.29 (35.0 %)
Elemental carbon (μg m ⁻³)	0.15 ± 0.08 (0.8 %)	0.15 ± 0.08 (0.9 %)	0.44 ± 0.28 (1.3 %)	0.51 ± 0.26 (1.9 %)
Unknown (μg m ⁻³)	2.52 ± 3.26 (14.0 %)	2.20 ± 3.40 (13.5 %)	4.11 ± 7.78 (12.1 %)	1.82 ± 4.48 (6.7 %)

3.1.1 Ship emission markers: V and Ni

Several studies focussed on the identification of shipping emission specific tracers (Viana et al., 2008; Becagli et al., 2012; Isakson et al., 2001; Hellebust et al., 2010). Vanadium and Nickel are generally considered the best markers for this source because, after sulfur, they are the main impurities in heavy fuel oil (Agrawal et al., 2008a, b). The soluble fraction of these metals is even more representative for ship sources (Becagli et al., 2012).

Following Becagli et al., (2012), we used measurements of the V and Ni soluble fractions (V_{sol} and Ni_{sol}, respectively). In the data set the V_{sol} and Ni_{sol} ratio with respect to Al was always more than 10 times larger than for UCC, as expected for cases dominated by heavy oil combustions sources (ships, refineries, power plants, stainless steel production plants).

Table 3 reports slope, correlation coefficient and number of samples of the linear correlation between V_{sol} and Ni_{sol}.

V_{sol} and Ni_{sol} are highly correlated, suggesting a common source. The obtained slope of the regression line (2.8–2.9, that increases to 3.0 for samples with V_{sol} > 6 ng m⁻³) is in the range of ratios typical for heavy fuel oil combus-

Table 3. Correlation parameters between V and Ni at LMP and CGR calculated for all the samples, and for samples with V concentration higher than 6 ng m⁻³.

		Slope (± uncertainty)	R ²	n
LMP	All data	2.94 ± 0.03	0.986	124
	V _{sol} > 6 ng m ⁻³	2.99 ± 0.03	0.994	44
CGR	All data	2.82 ± 0.08	0.950	59
	V _{sol} > 6 ng m ⁻³	3.00 ± 0.05	0.989	34

tion sources. The same value was found at Lampedusa by Becagli et al., (2012), considering data from 2004 to 2008. The behaviour of V, Ni and their ratio are then representative of heavy fuel oil combustion. It must be emphasized that the V / Ni ratio is expected to display a large variability due to varying fuel composition and engine operating conditions (Mazzei et al., 2008; Agrawal et al., 2008a, b; Viana et al., 2009; Pandolfi et al., 2011). It is however, difficult to distinguish V and Ni originating from power plants, refineries,

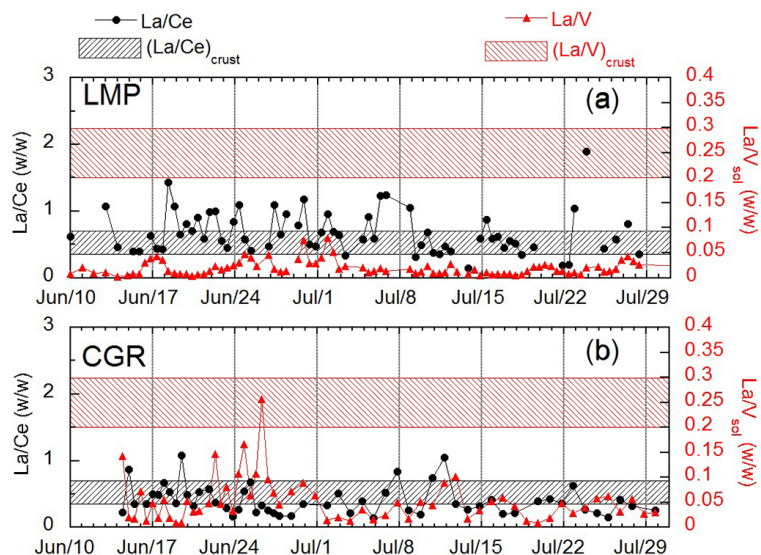


Figure 4. Time series of LCR and LVR at (a) LMP, and (b) CGR. The horizontal red and grey shadow areas in each plot represent the ranges of values for upper continental crust LVR and LCR, respectively.

or ship engines. Moreover, several refineries are present in Sicily (Siracusa, Gela, Milazzo) and in Sardinia (Cagliari) and may potentially influence the sampling sites.

A combination of methods is thus used in this study to unequivocally identify the ship source. The analysis is based on: additional chemical tracers, such as the rare earth elements, whose behaviour is specific for the refinery and the ship sources; high-resolution back-trajectories, based on data from the high-resolution regional model; information on the vertical mixing in the atmospheric boundary layer; and coincidences between the high-resolution back-trajectories and the position of different types of ships in the Strait of Sicily.

3.1.2 Rare earth elements

As discussed above, anthropogenic V and Ni originate from heavy oil combustion and may only be considered markers of the ship source when other sources can be excluded. Few studies propose the use of lanthanoid elements (La to Lu) to distinguish refinery from ship emissions (Moreno et al., 2008a, b; Du and Turner, 2015; Kulkarni et al., 2006).

In particular, the ratio between the La and Ce concentrations (La / Ce ratio, hereafter LCR) and between La and V (hereafter LVR) can be used to identify specific sources. Shipping emissions are characterised by values of LCR between 0.6 and 0.8 and $LVR < 0.1$ (Moreno et al., 2008a, b).

Crustal aerosols are characterized by LCR ranging from 0.4 to 0.6 and LVR usually in the range of 0.2–0.3 (Moreno et al., 2008a, b). LCR depends weakly on differences in dust source area and collected aerosol size fraction, contrarily to LVR, which reaches 0.9 for large ($> 10 \mu\text{m}$) particles from specific areas of the Sahara (e.g. Hoggar Mas-

sif; Henderson and Henderson, 2009; Moreno et al., 2006; Castillo et al., 2008).

Elevated values of LCR (from 1 to 13) are associated with emissions from refineries (Moreno et al., 2008a; Du and Turner, 2015). This is because zeolitic fluidised-bed catalytic cracking (FCC) units enriched in La are used to crack long-chain olefins in crude oil to shorter-chain products (Bozlake et al., 2013; Du and Turner, 2015; Kulkarni et al., 2006; Moreno et al., 2008a, b).

Mixing of aerosol from different sources may produce a large variability of LCR, with larger values corresponding to a stronger impact from refineries.

The time series of LCR and LVR at LMP and CGR are displayed in Fig. 4. The range of values expected for crustal aerosol is highlighted in the figure. Please, note that the uncertainty on LCR is very large when La and Ce concentrations are close to the detection limit. These cases may produce very large values of LCR which are not significant; and were removed from the time series.

LCR at LMP and CGR was generally around the value expected for crustal aerosol (dashed grey area in Fig. 4); 10 samples from LMP and 2 samples from CGR show values of LCR higher than 1. LCR is > 1.5 in a single case, at LMP. This suggests that the refineries impact is small in the collected samples.

Moreno et al. (2008b) have shown that it is possible to identify aerosol from refineries based on the V-La-Ce-three-component plot. This type of plot is shown in Fig. 5 for the data from LMP and CGR. La and Ce were scaled in order to have the typical UCC composition in the centre of the plot.

The compositions of UCC (Henderson and Henderson, 2009), African desert dust (Castillo et al., 2008; Moreno et

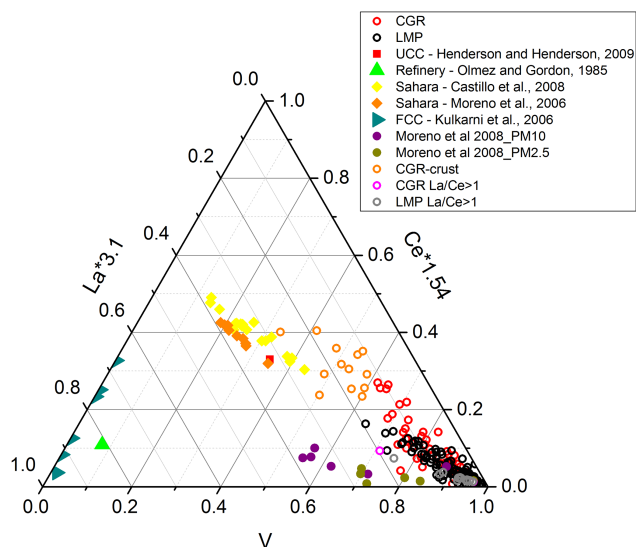


Figure 5. Three-component Ce-La-V plot for LMP and CGR. Literature data for different aerosol types are also shown.

al., 2006), FCC (Kulkarni et al., 2006), La-contaminated (refinery) Asian dust collected at Mauna Loa, Hawai'i (Olmez and Gordon, 1985), and PM₁₀ as well as PM_{2.5} that were collected at Puertollano (Spain) in days possibly affected by refinery emissions (Moreno et al., 2008b) are also displayed in Fig. 5.

The data from CGR and LMP are grouped in a region with elevated values of V, and La and Ce generally lower than in refinery and dust cases.

Data from Puertollano shown in Fig. 5 are relative to days characterized by winds originating from sectors where refineries are located; however, these samples are affected by a mix of particles from several sources, including refineries. Aerosol samples from Spain affected by refineries, in most cases display larger LCR and LVR ratios than those found at LMP and CGR. The composition of all samples collected in this period at LMP is consistent with a large impact from ship emissions. Some cases at CGR may suggest the simultaneous occurrence of crustal and ship aerosols, or dominant crustal components (orange open dots in Fig. 5). Therefore, these cases display a relatively low V concentration and are mainly associated with the mistral event. A limited crustal contamination may possibly occur at CGR in these cases, due to resuspension due to the strong wind.

Cases with LCR > 1 (grey and pink open circles for CGR and LMP respectively) are highlighted in Fig. 5. The aerosol composition is consistent, however, with the ship source in these cases, suggesting that the impact of refineries is limited.

3.2 Trajectories and ship traffic

3.2.1 Origin of air masses during the campaign

All the trajectories arriving at LMP and CGR, calculated with the HYSPLIT model driven by WRF meteorological fields (see Sect. 2.3), are shown in an aggregated way in Fig. 6, where the trajectory frequency at each point of the computing grid is shown for the whole period (upper panels) and for the 10–30 June interval (lower panels). The trajectory frequency pattern is elongated in the NW–SE direction at LMP, while it is distributed over a wider range of directions at CGR, despite a general prevalence of northerly sectors. The predominance of air masses coming from the northwest is particularly evident in June (Fig. 6c and d), when areas with trajectory frequencies exceeding 10% are found farther to the north, up to the Gulf of Lion.

During the first part of the campaign (June 2013) the synoptic situation was characterized by a “dipolar” sea level pressure anomaly pattern, with positive anomalies in the western Mediterranean and negative ones in the eastern part of the basin (Denjean et al., 2016). This situation induced stronger and more frequent than usual northwesterly winds (i.e. mistral episodes, see Sect. 3.1) over Sardinia and Strait of Sicily.

3.2.2 Ship traffic

To further investigate the mechanisms determining the presence of ship emissions markers at the two sites, we investigated the relationships among the amount of V, the back-trajectory pattern, the effective number of ships influencing the air mass, the stability of the boundary layer in the ship source region (i.e. the Strait of Sicily) and the REE to V ratios discussed in Sect. 3.1.2.

All back-trajectories arriving at LMP and CGR were considered and all trajectory-ship coincidences occurring within the last 36 hours before sampling were taken into account.

It was assumed that the ship plume influenced the sampled air mass if:

- the trajectory passed within 15 km of the position of a ship;
- the corresponding air mass altitude was less than 500 m.

The total number of ships fulfilling these criteria was associated with each trajectory. The analysis was based on the available 1 h time resolution meteorological fields (a ship influencing a trajectory was counted once every hour).

To further explore the impact of different types of ships, the analysis was carried out considering the following three ship categories: all the ships, the merchant (i.e. cargo and tanker) and the fishing vessels.

The atmospheric stability is also expected to play a large role in modulating the ship impact (for an example of its influence on V amounts, see Becagli et al., 2012). A temper-

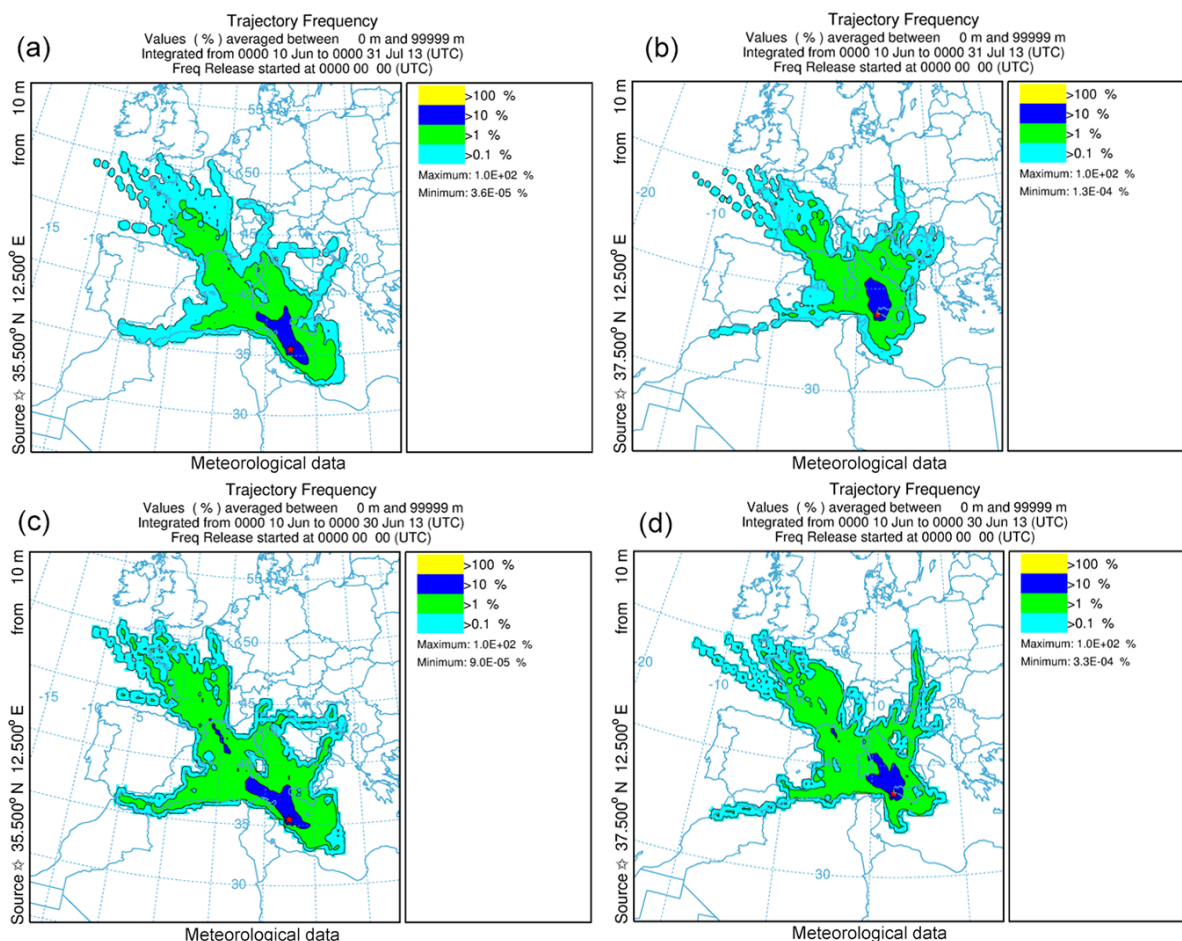


Figure 6. Trajectory frequency computed at each grid cell with starting points at LMP (a, c) and CGR (b, d). Upper panels show values averaged over the whole period of the campaign (10 June–31 July 2013), while lower panels are relative to the 10–30 June interval.

ature inversion (TI) index was calculated based on the 3-D atmospheric fields of the WRF model at three sites in the Strait of Sicily. The temperature inversions were used as a proxy to identify periods characterized by a stable boundary layer. The three sites, A (37.2° N, 11.5° E), B (37.0° N, 12.4° E) and C (36.3° N, 13.3° E) (Fig. 1) were selected in the regions of most frequent ship passage and crossing with the trajectories from LMP and CGR. The TI index was calculated as the difference between the temperature at the altitude of the maximum, T , and at the surface. A positive TI indicates an inversion and the TI value provides an indication of the inversion strength. Only positive values are considered in this analysis.

Figure 7 summarizes the results of this analysis. It shows the time series of the number of the ships influencing the trajectories arriving at LMP and CGR, respectively, and the corresponding measured values of V . Samples which show a limited influence from ship emissions, determined on the basis of the La-Ce-V composition (see Sect. 3.1.2), are highlighted with arrows (orange arrows for samples with La-Ce-

V ratios typical for crust; pink and gray for sample possibly influenced by refineries, i.e. with $LCR > 1$). Results are shown for the three classes of ships. The positive values of TI are also shown.

In general, there is a rather good correspondence between the cases classified as influenced by ships emissions and the number of ships encountered along the associated air mass trajectory at CGR. The correspondence is somewhat less evident at LMP. As discussed above, the V concentration ascribed to ships (data points without arrows in Fig. 7) is generally higher at CGR than at LMP. Part of this difference may be ascribed to the shorter distance between CGR and the main shipping route crossing the Strait of Sicily with respect to LMP, the consequent larger number of encountered ships and an aerosol dilution effect during transport from the sources to LMP.

Maxima of V attributed to ships occurred between 19 and 20 June at CGR (about 42 ng m^{-3}) and on 21 June at LMP (36.1 ng m^{-3}). Similar concentrations were measured at CGR also around 18–19 July, in conjunction with an in-

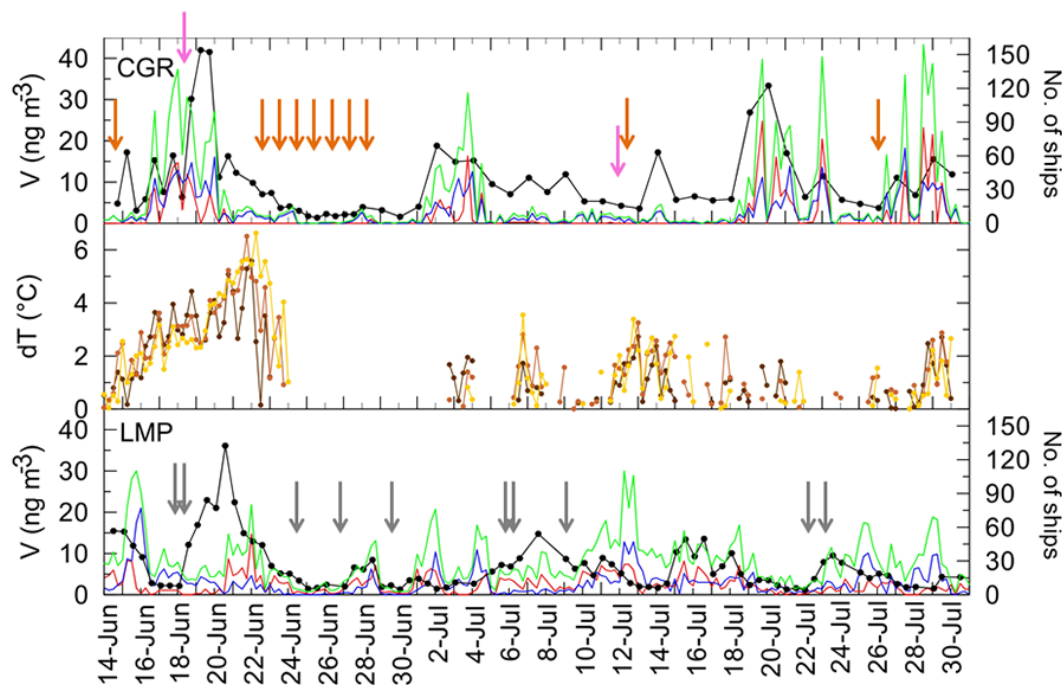


Figure 7. Time series of Vanadium concentration (black line with dots) and number of ships affecting the air masses sampled at CGR (upper panel) and LMP (lower panel). Green, red and blue lines indicate, respectively, the total number of ships and the number of merchant (i.e. cargo and tanker) and fishing vessels. The time evolution of the temperature inversion index (dT in the figure) at three different locations in the Strait of Sicily is shown in the middle panel; brown, red and yellow curves show the behaviour at sites A–C (see text). The orange arrows identify samples classified as crustal, based on the La-Ce-V concentration; pink and gray arrows identify samples with $LCR > 1$, possibly influenced by refineries.

crease in the number of merchant vessels. The 18–21 June period is the only event with high V concentrations quasi simultaneously at both sites. This is due to the peculiar circulation patterns, with air mass trajectories from the marine sector south of Sicily to CGR, and from the Strait of Sicily to LMP, particularly on 18 and 19 June. The 19–21 June episode is the largest occurring at LMP, both for duration and V concentration. Especially at the beginning of the event, large values of V do not correspond with an increase of the number of ships along the air mass trajectories.

A possible explanation for this behaviour is provided by the temporal evolution of TI in the Strait of Sicily. The temperature inversion started to develop on 14 June and gradually increased in intensity until 22 June; the TI persistence and progressive increase in intensity provided suitable conditions for the ship plumes being trapped in the boundary layer, with a consequent build-up of the ship aerosol and V concentration. This process appears particularly efficient at CGR between 21 and 25 June.

A similar combined dependency on number of ships and TI appears also at LMP around 7 July. It is interesting to note that V from ships seems to depend more directly on the number of merchant ships (see, for example, the lack of V peaks on 17 June, 12 and 29 July at LMP, when the number

of fishing vessels was high and the number of merchant ships was low) than on the total or the number of fishing ships.

Thus, the trajectory analysis, carried out in combination with the available information on the ship tracks, confirms that ship emissions are the main factors responsible for most of the moderate and elevated values of V measured at LMP and CGR during the campaign and in particular for those cases with LCR compatible with the ship source. This analysis also clearly suggests that the boundary layer structure plays a very important role in determining the impact produced by the emissions. This simplified approach confirms the importance of carefully characterizing the emission scenario and the meteorological conditions in studies on the ships' emissions impact on air quality.

3.3 Sulfate, nitrate and organic carbon from ships

SO₂ is one of the main species emitted in the ship plume in the gas phase (Agrawal et al., 2008a, b). SO₂ is produced through oxidation of the S contained as impurity in heavy fuel oil and is an aerosol precursor.

A previous study based on five years of data from Lampedusa (Becagli et al., 2012) has shown that the non-sea salt sulfate behaviour is not directly correlated with V and Ni because several other SO₄²⁻ sources (anthropogenic, marine

biogenic, crustal, volcanic) contribute to the non-sea salt sulfate in the Central Mediterranean Sea.

The same study suggested a lower limit of about 200 for the nssSO_4^{2-} / V ratio for particles originating from heavy oil combustion at Lampedusa.

Figure 8a and 8b shows nssSO_4^{2-} / V vs. V at LMP and CGR. At both sites, nssSO_4^{2-} / V decreases with increasing V and reaches a lower limit at elevated values of V ($> 15 \text{ ng m}^{-3}$). The analysis on REE, trajectories and ship traffic has shown that all samples with $V > 15 \text{ ng m}^{-3}$ are strongly influenced by ships and we assume that ship emission is the dominant source of the sampled particles for these cases. This implies that in these cases virtually all sulfate originated from the ship source and the observed lower limit for nssSO_4^{2-} / V can be considered the lower limit for the sulfate to V ratio in the ship plume. Thus, to derive a lower limit for this ratio we calculate the mean and standard deviation of nssSO_4^{2-} / V for $V > 15 \text{ ng m}^{-3}$. The mean ratio and the mean ratio minus one standard deviation are shown in Fig. 8.

The nssSO_4^{2-} to V ratio may still be decreasing for V by around 15 ng m^{-3} , and we used a limit value equal to the average minus one standard deviation (solid red lines in Fig. 8) to estimate the minimum expected contribution from ships to the total sulfate amount.

The calculated lower limit of the sulfate to V ratio at LMP is 207, in agreement with the values of 200 estimated by Becagli et al., (2012). The nssSO_4^{2-} / V limit value at CGR, 323, is larger than at LMP. This difference may be due to the contribution of other sulfate sources, which may contribute to the nssSO_4^{2-} , even at high V concentration, and to the smaller distance from the ship source with respect to LMP. This result highlights the importance of remote sites like LMP to obtain information on the open Mediterranean.

NO_x are among the main compounds emitted in the gas phase acting as aerosol precursors. The photochemistry of NO_x leading to NO_3^- formation in the particulate phase is complex, especially in summer, due to the presence of high amounts of OH radical (see, for example, Chen et al., 2005), and the NO_x contribution to the particulate phase is not easy to be quantified.

Here we try to use the same approach used for sulfate for the determination of a lower limit for the NO_3^- / V ratio in the ship plume.

Figure 8c and d show the NO_3^- / V ratio vs. V at the two sites. Similarly to sulfate, the average value of NO_3^- / V for $V > 15 \text{ ng m}^{-3}$ is larger at CGR than at LMP. However, the standard deviation at CGR is significantly larger at CGR. The NO_x concentration in the ship plume close to the source is larger than that of SO_2 and is strongly dependent on the engine operating conditions (Agrawal et al., 2008b). The NO_x lifetime is extremely low (1.8 h during the daytime and 6.5 h during the nighttime, Chen et al., 2005). However, the NO_3^- / V limit ratio values is low compared to the limit ratio for SO_4^{2-} . It has to be considered that NO_3^- takes part in

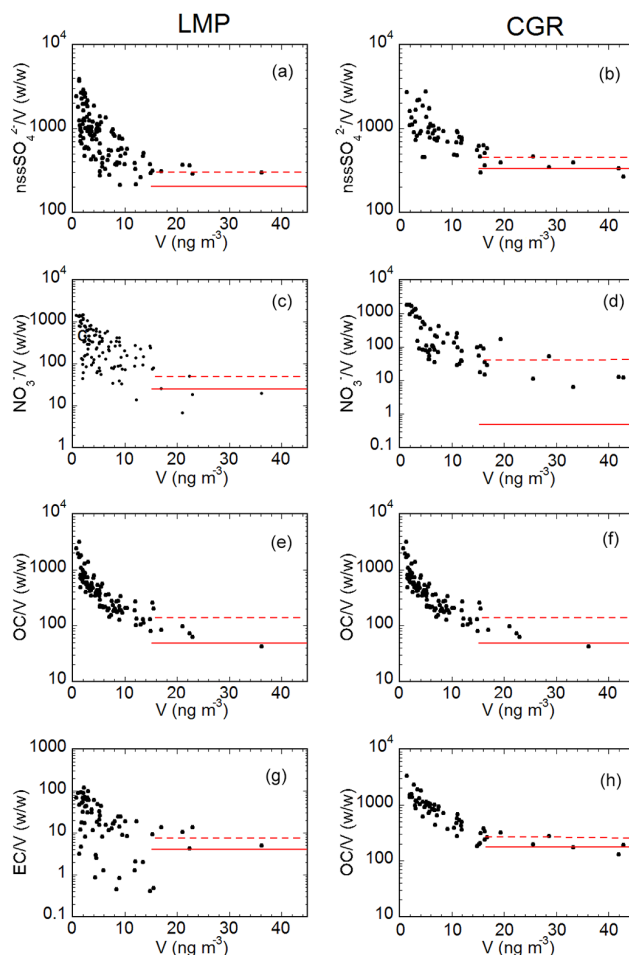


Figure 8. Scatter plots of nssSO_4^{2-} / V (a, b), NO_3^- / V (c, d), OC / V (e, f) and EC / V (g, h) vs. V concentration at LMP (plots on the left) and CGR (plots on the right). The red lines in the plots represent the average (dashed line) and the average minus one standard deviation (solid line) calculated for samples with $V > 15 \text{ ng m}^{-3}$.

other photochemical atmospheric reactions that lead to its removal. In addition, the presence of HNO_3 in the gas phase, not neutralized by NH_3 or by sea salt, could explain the low $\text{NO}_3^- / \text{nssSO}_4^{2-}$ ratio in the aerosol. Indeed, the NO_3^- concentration measured at LMP and CGR is four to six times lower than that of nssSO_4^{2-} (Table 1). Low amounts of NO_3^- , with respect to SO_4^{2-} from ship emissions, are found in model simulations in southern California (Dabdub, 2008). Indeed, Dabdub (2008) shows that the aerosol contribution from ship emissions is 0.05 % for NO_3^- and 44 % for SO_4^{2-} .

Elemental and Organic Carbon are also present in the ship plume (Shah et al., 2004). In particular, OC constitutes about 15–25 % and EC is generally lower than 1 % of the PM sampled at the plume of main ship engine powered by heavy fuel oil (Agrawal et al., 2008b).

Figure 8 shows EC / V and OC / V vs. V at LMP and CGR. Similarly to sulfate and nitrate, OC / V de-

Table 4. Estimates of the average and maximum of the lower limit of nssSO_4^{2-} , NO_3^- , OA and PM_{10} from ships. Concentrations and percent with respect to the total amount of each species are reported. The maxima are derived by selecting cases with the largest ship impact (i.e. highest V concentration).

	nssSO_4^{2-} (nssSO_4^{2-} / V) _{min} = 207		NO_3^- (NO_3^- / V) _{min} = 12.5		OA (OC / V) _{min} = 43.1		PM_{10}	
	LMP	CGR	LMP	CGR	LMP	CGR	LMP	CGR
Average contribution $\mu\text{g m}^{-3}$ (%)	1.35 (34 %)	2.1 (31 %)	0.082 (4.5 %)	0.13 (9.0 %)	0.59 (15 %)	0.78 (8.7 %)	2.0 (11 %)	3.0 (8.6 %)
Maximum contribution $\mu\text{g m}^{-3}$ (%)	7.5 (69 %)	8.8 (77 %)	0.45 (62 %)	0.53 (100 %)	3.3 (99 %)	3.3 (22 %)	11.2 (50 %)	12.7 (42 %)

creases with increasing V and reaches a minimum value for $V > 15 \text{ ng m}^{-3}$ (43.1 and 179 at LMP and CGR, respectively) As discussed in Sect. 3.1, other OC sources in addition to ships are present at CGR even at high values of V.

The pattern of the ratio EC / V vs. V is less clear; in particular, several very low values of EC / V also appear at small values of V. This result is unexpected because V and EC are both markers of the primary ship aerosol, but the data here presented seem to suggest that non negligible EC contributions from other sources were present at CGR and that different fractionating effects acted during the transport. Also in this case the limit value is lower at LMP than at CGR.

Finally, as the limit ratios at CGR are likely affected by other sources than shipping, we assume that the limit ratios obtained at Lampedusa for $V > 15 \text{ ng m}^{-3}$ are more representative of cases dominated by ship emissions during summer in a wide region. For this reason, the retrieved lower limits at LMP are also used to quantify the ship contribution at CGR.

3.4 Contribution of the ship aerosol to PM_{10}

With all the limitations described above, by using the lower limits for the ratios nssSO_4^{2-} / V , NO_3^- / V and OC / V (representative for ship aerosol) it is possible to estimate the minimum contribution of nssSO_4^{2-} , NO_3^- and OC emitted by ships to the total budget of these components and also to the total PM_{10} mass. It has to be noticed that the aerosol quantification obtained by this method is a rough estimate useful to constrain the ship aerosol contribution. In addition, due to possibly different meteorological conditions and photochemical activity, these values may vary spatially and seasonally.

The minimum ratio of each species with respect to V and the minimum estimated contribution of ship emissions, for the average amount and for the maxima, of the total concentration of these species and of PM_{10} are reported in Table 4. As previously discussed, the measured OC contribution is

multiplied by 2.1 at LMP and by 1.8 at CGR to obtain the total organic aerosol contribution.

The estimated minimum concentration of non-sea-salt sulfate from ship emissions was $1.35 \mu\text{g m}^{-3}$ on average during this campaign at LMP. This value is lower than in the previous study by Becagli et al., (2012) obtained over a longer period (2004–2008). The relative contribution to the total sulfate is, however, similar here and in Becagli et al., (2012), suggests a similar role of nssSO_4^{2-} from ship emissions to the total nssSO_4^{2-} budget. The study by Becagli et al., (2012) covered an extended time period (2004–2008); the consistency with that study suggests that the results obtained during ChArMEx are not specific of summer 2013, but are representative for a wider temporal and spatial range.

At CGR the minimum ship contribution to sulfate, averaged over the same time period, is higher than at LMP ($2.1 \mu\text{g m}^{-3}$), but this higher value corresponds to a lower contribution to the total nssSO_4^{2-} , confirming that other nssSO_4^{2-} sources are important at CGR.

Marmer and Langmann (2005) estimate that ship emissions contribute by 50 % to the total amount of nssSO_4^{2-} in the Mediterranean. This value is, as expected, larger than the estimated minimum contribution we derive (about 30 %).

The estimated minimum contribution by ships to the total nssSO_4^{2-} for cases with the largest ship impact (i.e. highest V concentration) is 69 and 77 % at LMP and CGR, respectively.

Ships appear to contribute, by small fractions, to the total budget of NO_3^- . As previously mentioned, the NO_3^- atmospheric chemistry is complex and the contribution of nitrate from ship emission could be highly variable, especially in the Mediterranean region where high amounts of UV radiation and highly reactive radical species are present.

Organic aerosol from ships also contributes significantly to the total OA amount and to the total PM; in particular, at LMP virtually all the OA present in cases with maximum ship impact may be attributed to the ship source.

By summing these three contributions, it is possible to estimate the total aerosol mass due to ship emissions and its contribution to the total mass of PM_{10} . The lower limit for the ship contribution was 2.0 and $3.0 \mu\text{g m}^{-3}$, corresponding to 11 and 8.6 % of PM_{10} at LMP and CGR, respectively.

These percent contributions are higher than the annual average for the Mediterranean region estimated by Viana et al., (2014). It has to be considered that these authors used data from harbour or coastal sites, which are highly affected by other sources in addition to ships, and where gas-to-particle conversion is still at its initial phase. Moreover, the percentages reported in this study are relative to the summer season, when the ship contribution in the Mediterranean region is highest (Becagli et al., 2012).

The estimated lower limit for the ship contribution in cases with maximum ship impact was between 42 and 50 % of the total PM_{10} .

4 Summary and conclusions

In this study we have investigated the impact of the ship emissions to PM_{10} on measurements made at two sites in the central Mediterranean. The main objectives of the study were to unambiguously identify the tracers of ship emissions in the sampled aerosol and to obtain a lower limit for the produced impact.

The PM_{10} samples were collected in summer 2013, as a contribution to the Chemistry and Aerosol Mediterranean Experiment, in parallel at LMP and at CGR, respectively, south and north of the main shipping route through the Mediterranean.

The identification of aerosol originating from ships was based on an integrated analysis combining chemical analyses, calculations of backward trajectories using a high resolution regional model and on tracking of ship traffic in the Mediterranean through the Automatic Identification System.

The main results of this study may be summarized as follows:

1. Moderate and elevated values of V and Ni in the aerosol were unambiguously associated with the ship source; this attribution was based on:
 - the V to Ni ratio, which corresponds to what is expected for heavy fuel oil combustion;
 - low amounts of La and Ce with respect to V and La / Ce ratios similar to those in the UCC, which allowed the exclusion of power plants or refineries as sources significantly contributing to the observed aerosol;
 - coincidences between air mass trajectories and travelling ships.
2. In addition to travelling ships, also the planetary boundary layer vertical structure played an important role in

determining the dispersion of aerosols from the ship source; temperature inversions appeared associated with elevated amounts of ship emissions tracers, suggesting that they favoured the build-up of aerosol concentration in the lowest atmospheric layers.

3. As expected, merchant ships (cargo and tankers) appeared to produce a larger impact on the measured aerosol than fishing vessels.
4. Lower limits for the ratios $\text{nssSO}_4^{2-} / \text{V}$, NO_3^- / V , and OC / V , identifying the ship-dominated emission cases, were derived from the observations. The lower limits found at Lampedusa, which may be taken as a background site less affected by other types of anthropic emissions, are respectively 207, 12.5 and 44.1. These lower limits are expected to be season dependent.
5. By using these ratios, the lower limits to the contribution of the ship source to nssSO_4^{2-} , NO_3^- , OA, and to PM_{10} during the measurement campaign were estimated. Ship emissions contributed to the total amount of sulfate by at least 34 %, to the total amount of NO_3^- by at least 5–9 %, and to the total amount of organic aerosol by at least 9–15 %. All these contributions correspond at least to 11 % of PM_{10} at LMP ($2.0 \mu\text{g m}^{-3}$), and about 8.6 % of PM_{10} at CGR ($3.0 \mu\text{g m}^{-3}$). In cases with largest ship impact, ships contributed up to about $12 \mu\text{g m}^{-3}$ to PM_{10} in both sites, corresponding to 50 % of PM_{10} at LMP and 42 % at CGR.
6. Lampedusa is a small island in the southern sector of the central Mediterranean, relatively far from the main Mediterranean shipping route; thus, results at Lampedusa may be taken as representative of the impact of ships on the aerosol properties in a wide open sea area in the central Mediterranean during summer.

5 Data availability

All the data presented in this paper are available upon request. Please contact the corresponding author (silvia.becagli@unifi.it).

Competing interests. The authors declare that they have no conflict of interest.

Acknowledgements. Measurements at Lampedusa were partly supported by the Italian Ministry for University and Research through the NextData and Ritmare projects.

We thank the Institute for Coastal Marine Environment of the National Research Council (IAMC-CNR) for hosting the instruments at Capo Granitola. Thanks are due to MarineTraffic (<http://www.marinetraffic.com>) for providing the information on the ship traffic in the Strait of Sicily.

Edited by: M. Beekmann

Reviewed by: two anonymous referees

References

- Agrawal, H., Malloy, Q. G. J., Welch, W. A., Miller, J. W., and Cocker, D. R.: In-use gaseous and particulate matter emissions from a modern ocean going container vessel, *Atmos. Environ.*, 42, 5504–5510, 2008a.
- Agrawal, H., Welch, W. A., Miller, J. W., and Cocker, D. R.: Emission measurements from a crude oil tanker at sea, *Environ. Sci. Technol.*, 42, 7098–7103, 2008b.
- Artuso, F., Chamard, P., Piacentino, S., Sferlazzo, D. M., De Silvestri, L., di Sarra, A., Meloni, D., and Monteleone, F.: Influence of transport and trends in atmospheric CO₂ at Lampedusa, *Atmos. Environ.*, 43, 3044–3051, 2009.
- Ault, A. P., Gaston, C. J., Wang, Y., Dominguez, G., Thiemens, M. H., and Prather, K. A.: Characterization of the single particle mixing state of individual ship plume events measured at the port of Los Angeles, *Environ. Sci. Technol.*, 44, 1954–1961, 2010.
- Becagli, S., Sferlazzo, D. M., Pace, G., di Sarra, A., Bommarito, C., Calzolari, G., Ghedini, C., Lucarelli, F., Meloni, D., Monteleone, F., Severi, M., Traversi, R., and Udisti, R.: Evidence for heavy fuel oil combustion aerosols from chemical analyses at the island of Lampedusa: a possible large role of ships emissions in the Mediterranean, *Atmos. Chem. Phys.*, 12, 3479–3492, doi:10.5194/acp-12-3479-2012, 2012.
- Becagli, S., Lazzara, L., Fani, F., Marchese, C., Traversi, R., Severi, M., di Sarra, A., Sferlazzo, D., Piacentino, S., Bommarito, C., Dayan, U., and Udisti, R.: Relationship between methanesulfonate (MS-) in atmospheric particulate and remotely sensed phytoplankton activity in oligo-mesotrophic Central Mediterranean Sea, *Atmos. Environ.*, 79, 681–688, 2013.
- Bove, M. C., Brotto, P., Cassola, F., Cuccia, E., Massabò, D., Mazzino, A., Piazzalunga, A., and Prati, P.: An integrated PM_{2.5} source apportionment study: Positive Matrix Factorization vs. the Chemical Transport Model CAMx, *Atmos. Environ.*, 94, 274–286, doi:10.1016/j.atmosenv.2014.05.039, 2014.
- Bove, M. C., Brotto, P., Calzolari, G., Cassola, F., Cavalli, F., Fermo, P., Hjorth, J., Massabò, D., Nava, S., Piazzalunga, A., Schembari, C., and Prati, P.: PM₁₀ source apportionment applying PMF and chemical tracer analysis to ship-borne measurements in the Western Mediterranean, *Atmos. Environ.*, 125, 140–151, doi:10.1016/j.atmosenv.2015.11.009, 2016.
- Bowen, H. J. M.: *Environmental chemistry of the elements*, Academic Press, London, New York, 1979.
- Bozlaker, A., Buzcu-Güven, B., Fraser, M. P., and Chellam, S.: Insights into PM₁₀ source in Houston, Texas: Role of Petroleum refineries in enriching lanthanoid metal during episodic emission events, *Atmos. Environ.*, 69, 109–117, doi:10.1016/j.atmosenv.2012.11.068, 2013.
- Calzolari, G., Nava, S., Lucarelli, F., Chiari, M., Giannoni, M., Becagli, S., Traversi, R., Marconi, M., Frosini, D., Severi, M., Udisti, R., di Sarra, A., Pace, G., Meloni, D., Bommarito, C., Monteleone, F., Anello, F., and Sferlazzo, D. M.: Characterization of PM₁₀ sources in the central Mediterranean, *Atmos. Chem. Phys.*, 15, 13939–13955, doi:10.5194/acp-15-13939-2015, 2015.
- Canepari, S., Farao, C., Marconi, E., Giovannelli, C., and Perrino, C.: Qualitative and quantitative determination of water in airborne particulate matter, *Atmos. Chem. Phys.*, 13, 1193–1202, doi:10.5194/acp-13-1193-2013, 2013.
- Casasanta, G., di Sarra, A., Meloni, D., Monteleone, F., Pace, G., Piacentino, S., and Sferlazzo, D.: Large aerosol effects on ozone photolysis in the Mediterranean, *Atmos. Environ.*, 45, 3937–3943, 2011.
- Cassola, F., Ferrari, F., Mazzino, A., and Miglietta, M. M.: The role of the sea on the flash floods events over Liguria (northwestern Italy), *Geophys. Res. Lett.*, 43, 3534–3542, doi:10.1002/2016GL068265, 2016.
- Castillo, S., Moreno, T., Querol, X., Alastuey, A., Cuevas, E., Herrmann, L., Mounkaila, M., and Gibbons, W.: Trace element variation in size-fractionated African desert dusts, *J. Arid Environ.*, 72, 1034–1045, doi:10.1016/j.jaridenv.2007.12.007, 2008.
- Cesari, D., Genga, A., Ielpo, P., Siciliano, M., Mascolo, G., Grasso, F. M., and Contini, D.: Source apportionment of PM_{2.5} in the harbour-industrial area of Brindisi (Italy): Identification and estimation of the contribution of in-port ship emissions, *Sci. Total Environ.*, 497–498, 392–400, 2014.
- Chen, G., Huey, G., and Trainer, M.: An investigation of the chemistry of ship emission plumes during ITCT 2002, *J. Geophys. Res.*, 110, D10S90, doi:10.1029/2004JD005236, 2005.
- Coakley Jr., J. A. and Walsh, C. D.: Limits to the aerosol indirect radiative effect derived from observations of ship tracks, *J. Atmos. Sci.*, 59, 668–680, 2002.
- Contini, D., Gambaro, A., Belosi, F., Pieri, S. D., Cairns, W. R. L., Donato, A., Zanutto, E., and Citron, M.: The direct influence of ship traffic on atmospheric PM_{2.5}, PM₁₀ and PAH in Venice, *J. Environ. Manage.*, 92, 2119–2129, 2011.
- Cooper, D. A.: Exhaust emissions from ships at berth, *Atmos. Environ.*, 37, 3817–3830, 2003.
- Corbett, J. J., Winebrake, J. J., Green, E. H., Kasibhatla, P., Eyring, V., and Lauer, A.: Mortality from Ship Emissions: A Global Assessment, *Environ. Sci., Technol.*, 41, 8512–8518, doi:10.1021/es071686z, 2007.
- Dabdub, D.: Air quality impacts of ship emission in south coast air basin of California, Final report for State of California Air Resources Board Planning and Technical support division, Sacramento, CA, available at: http://albeniz.eng.uci.edu/dabdub/My_Reports/R007_ARB_04-752.pdf (last access: February 2017), 2008.
- Denjean, C., Cassola, F., Mazzino, A., Triquet, S., Chevaillier, S., Grand, N., Bourrienne, T., Momboisse, G., Sellegri, K., Schwarzenbock, A., Freney, E., Mallet, M., and Formenti, P.: Size distribution and optical properties of mineral dust aerosols transported in the western Mediterranean, *Atmos. Chem. Phys.*, 16, 1081–1104, doi:10.5194/acp-16-1081-2016, 2016.
- Derwent, R., Stevenson, D. S., Doherty, R. M., Collins, W. J., Sanderson, M. G., Amann, M., and Dentener, F.: The contribution from ship emissions to air quality and acid deposition in Europe, *Ambio*, 34, 54–59, 2005.
- Devasthale, A., Krüger, O., and Graßl, H.: Impact of ship emissions on cloud properties over coastal areas, *Geophys. Res. Lett.*, 33, L02811, doi:10.1029/2005GL024470, 2006.
- Diesch, J.-M., Drewnick, F., Klimach, T., and Borrmann, S.: Investigation of gaseous and particulate emissions from various marine vessel types measured on the banks of the Elbe in Northern Ger-

- many, *Atmos. Chem. Phys.*, 13, 3603–3618, doi:10.5194/acp-13-3603-2013, 2013.
- di Sarra, A., Di Biagio, C., Meloni, D., Monteleone, F., Pace, G., Pugnaghi, S., and Sferlazzo, D.: Shortwave and longwave radiative effects of the intense Saharan dust event of 25–26 March, 2010, at Lampedusa (Mediterranean sea), *J. Geophys. Res.*, 116, D23209, doi:10.1029/2011JD016238, 2011.
- di Sarra, A., Sferlazzo, D., Meloni, D., Anello, F., Bommarito, C., Corradini, S., De Silvestri, L., Di Iorio, T., Monteleone, F., Pace, G., Piacentino, S., and Pugnaghi, S.: Empirical correction of MFRSR aerosol optical depths for the aerosol forward scattering and development of a long-term integrated MFRSR-Cimel dataset at Lampedusa, *Appl. Optics*, 54, 2725–2737, 2015.
- Donateo, A., Gregoris, E., Gambaro, A., Merico, A., Giua, R., Noci, A., and Contini, D.: Contribution of harbour activities and ship traffic to PM_{2.5}, particle number concentrations and PAHs in a port city of the Mediterranean Sea (Italy), *Environ. Sci. Pollut. Res.*, 21, 9415–9429, doi:10.1007/s11356-014-2849-0, 2014.
- Du, L. and Turner, J.: Using PM_{2.5} lanthanoid elements and nonparametric wind regression to track petroleum refinery FCC emissions, *Sci. Total. Environ.*, 529, 65–71, doi:10.1016/j.scitotenv.2015.05.034, 2015.
- Endresen, Ø., Sørsgård, E., Sundet, J. K., Dalsøren, S. B., Isaksen, I. S. A., Berglen, T. F., and Gravir, G.: Emissions from international sea transportation and environmental impact, *J. Geophys. Res.*, 108, 4560, doi:10.1029/2002JD002898, 2003.
- Environmental Modeling Center: The GFS Atmospheric Model, NCEP Office Note 442, National Oceanic and Atmospheric Administration, Global Climate and Weather Modeling Branch, Camp Springs, Maryland, 14 pp., available at: <http://www.emc.ncep.noaa.gov/officenotes/newernotes/on442.pdf> (last access: February 2017), 2003.
- Eyring, V., Koehler, H. W., van Aardenne, J., and Lauer, A.: Emissions from international shipping: 1. The last 50 years, *J. Geophys. Res.*, 110, D17305, doi:10.1029/2004JD005619, 2005.
- Gariazzo, C., Papaleo, V., Pelliccioni, A., Calori, G., Radice, P., and Tinarelli, G.: Application of a Lagrangian particle model to assess the impact of harbour, industrial and urban activities on air quality in the Taranto area, Italy, *Atmos. Environ.*, 41, 6432–6444, 2007.
- Grewal, D. and Haugstetter, H.: Capturing and sharing knowledge in supply chains in the maritime transport sector: critical issues, *Mar. Policy Manage.*, 34, 169–183, 2007.
- Hellebust, S., Allanic, A., O'Connor, I. P., Jourdan, C., Healy, D., and Sodeau, J. R.: Sources of ambient concentrations and chemical composition of PM_{2.5-0.1} in Cork Harbour, Ireland, *Atmos. Res.*, 95, 136–149, 2010.
- Henderson, P. and Henderson, G. M.: *The Cambridge Handbook of Earth Science Data*, Cambridge, University Press, Cambridge, 42–44, 2009.
- Henne, S., Brunner, D., Folini, D., Solberg, S., Klausen, J., and Buchmann, B.: Assessment of parameters describing representativeness of air quality in-situ measurement sites, *Atmos. Chem. Phys.*, 10, 3561–3581, doi:10.5194/acp-10-3561-2010, 2010.
- Isakson, J., Persson, T. A., and Lindgren, E. S.: Identification and assessment of ship emissions and their effects in the harbour of Goteborg, Sweden, *Atmos. Environ.*, 35, 3659–3666, 2001.
- Jiang, Q., Smith, R. B., and Doyle, J.: The nature of the mistral: Observation and modelling of two MAP events, *Q. J. Roy. Meteorol. Soc.*, 129, 857–875, 2003.
- Jonsson, A. M., Westerlund, J., and Hallquist, M.: Size-resolved particle emission factors for individual ships, *Geophys. Res. Lett.*, 38, L13809, doi:10.1029/2011GL047672, 2011.
- Kouvarakis, G., Tsigaridis, K., Kanakidou, M., and Mihalopoulos, N.: Temporal variations of surface regional background ozone over Crete Island in the southeast Mediterranean, *J. Geophys. Res.*, 105, 4399–4407, 2000.
- Kulkarni, P., Chellam, S., and Fraser, M. P.: Lanthanum and lanthanides in atmospheric fine particles and their apportionment to refinery and petrochemical operations in Houston, TX, *Atmos. Environ.*, 40, 508–520, doi:10.1016/j.atmosenv.2005.09.063, 2006.
- Lauer, A., Eyring, V., Hendricks, J., Jöckel, P., and Lohmann, U.: Global model simulations of the impact of ocean-going ships on aerosols, clouds, and the radiation budget, *Atmos. Chem. Phys.*, 7, 5061–5079, doi:10.5194/acp-7-5061-2007, 2007.
- Li, Z. and Aneja, V. P.: Regional analysis of cloud chemistry at high elevations in the eastern United States, *Atmos. Environ.*, 26A, 2001–2017, 1992.
- Lloyd's Register Engineering Services: Marine Exhaust Emissions Research Programme, London, 63 pp., 1995.
- Lyyränen, J., Jokiniemi, J., Kauppinen, E. I., and Joutsensaari, J.: Aerosol characterisation in medium-speed diesel engines operating with heavy fuel oils, *J. Aerosol Sci.*, 30, 771–784, 1999.
- Mailler, S., Menut, L., di Sarra, A. G., Becagli, S., Di Iorio, T., Bessagnet, B., Briant, R., Formenti, P., Doussin, J.-F., Gómez-Amo, J. L., Mallet, M., Rea, G., Siour, G., Sferlazzo, D. M., Traversi, R., Udisti, R., and Turquety, S.: On the radiative impact of aerosols on photolysis rates: comparison of simulations and observations in the Lampedusa island during the ChArMEx/ADRI-MED campaign, *Atmos. Chem. Phys.*, 16, 1219–1244, doi:10.5194/acp-16-1219-2016, 2016.
- Mallet, M., Dulac, F., Formenti, P., Nabat, P., Sciare, J., Roberts, G., Pelon, J., Ancellet, G., Tanré, D., Parol, F., Denjean, C., Brogniez, G., di Sarra, A., Alados-Arboledas, L., Arndt, J., Auriol, F., Blarel, L., Bourrienne, T., Chazette, P., Chevassier, S., Claeys, M., D'Anna, B., Derimian, Y., Desboeufs, K., Di Iorio, T., Doussin, J.-F., Durand, P., Féron, A., Freney, E., Gaimoz, C., Goloub, P., Gómez-Amo, J. L., Granados-Muñoz, M. J., Grand, N., Hamonou, E., Jankowiak, I., Jeannot, M., Léon, J.-F., Maillé, M., Mailler, S., Meloni, D., Menut, L., Momboisse, G., Nicolas, J., Podvin, T., Pont, V., Rea, G., Renard, J.-B., Roblou, L., Schepanski, K., Schwarzenboeck, A., Sellegri, K., Sicard, M., Solmon, F., Somot, S., Torres, B., Totems, J., Triquet, S., Verdier, N., Verwaerde, C., Waquet, F., Wenger, J., and Zapf, P.: Overview of the Chemistry-Aerosol Mediterranean Experiment/Aerosol Direct Radiative Forcing on the Mediterranean Climate (ChArMEx/ADRI-MED) summer 2013 campaign, *Atmos. Chem. Phys.*, 16, 455–504, doi:10.5194/acp-16-455-2016, 2016.
- Marconi, M., Sferlazzo, D. M., Becagli, S., Bommarito, C., Calzolari, G., Chiari, M., di Sarra, A., Ghedini, C., Gómez-Amo, J. L., Lucarelli, F., Meloni, D., Monteleone, F., Nava, S., Pace, G., Piacentino, S., Ruggi, F., Severi, M., Traversi, R., and Udisti, R.: Saharan dust aerosol over the central Mediterranean Sea: PM₁₀ chemical composition and concentration versus optical

- columnar measurements, *Atmos. Chem. Phys.*, 14, 2039–2054, doi:10.5194/acp-14-2039-2014, 2014.
- Marmer, E. and Langmann, B.: Impact of ship emissions on Mediterranean summertime pollution and climate: A regional model study, *Atmos. Environ.*, 39, 4659–4669, 2005.
- Marmer, E., Dentener, F., Aardenne, J. V., Cavalli, F., Vignati, E., Velchev, K., Hjorth, J., Moldanovà, J., Fridell, E., Popovicheva, O., Demirdjian, B., Tishkova, V., Faccinnetto, A., and Focsa, C.: Characterisation of particulate matter and gaseous emissions from a large ship diesel engine, *Atmos. Environ.*, 43, 2632–2641, 2009.
- Mazzei F., D'Alessandro, A., Lucarelli, F., Nava, S., Prati, P., Valli, G., and Vecchi, R.: Characterization of particulate matter sources in an urban environment, *Sci. Total Environ.*, 401, 81–89, 2008.
- Meloni, D., Junkermann, W., di Sarra, A., Cacciani, M., De Silvestri, L., Di Iorio, T., Estellés, V., Gómez-Amo, J. L., Pace, G., and Sferlazzo, D. M.: Altitude-resolved shortwave and longwave radiative effects of desert dust in the Mediterranean during the GAMARF campaign: indications of a net daily cooling in the dust layer, *J. Geophys. Res.*, 120, 3386–3407, doi:10.1002/2014JD022312, 2015.
- Mentaschi, L., Besio, G., Cassola, F., and Mazzino, A.: Performance evaluation of WavewatchIII in the Mediterranean Sea, *Ocean Model.*, 90, 82–94, doi:10.1016/j.ocemod.2015.04.003, 2015.
- Micco, A. and Pérez, N.: Maritime transport costs and port efficiency, edited by: Bank, I.-A. D., Inter-american Development Bank, Santiago de Chile, p. 50, 2001.
- Mihalopoulos, N., Stephanou, E., Kanakidou, M., Pilitsidis, S. and Bousquet, P.: Tropospheric aerosol ionic composition in the Eastern Mediterranean region, *Tellus B*, 49, 1–13, 1997.
- Moldanovà, J., Fridell, E., Popovicheva, O., Demirdjian, B., Tishkova, V., Faccinnetto, A., and Focsa, C.: Characterisation of particulate matter and gaseous emissions from a large ship diesel engine, *Atmos. Environ.*, 43, 2632–2641, 2009.
- Moreno, T., Querol, X., Alastuey, A., Pey, J., Cruzmiquillon, M., Perez, N., Bernabe, R., Blanco, S., Cardenas, B., and Gibbons, W.: Lanthanoid geochemistry of urban atmospheric particulate matter, *Environ. Sci. Technol.*, 42, 6502–6507, 2008a.
- Moreno, T., Querol, X., Alastuey, A., and Gibbons, W.: Identification of FCC refinery atmospheric pollution events using lanthanoid- and vanadium-bearing aerosols. *Atmos. Environ.*, 42, 7851–7861, doi:10.1016/j.atmosenv.2008.07.013, 2008b.
- Moreno, T., Querol, X., Castillo, S., Alastuey, A., Cuevas, E., Herrmann, L., Mounkaila, M., Elvira, J., and Gibbons, W.: Geochemical variation in aeolian mineral particles from the Sahara-Sahel dust corridor, *Chemosphere*, 65, 261–270, doi:10.1016/j.chemosphere.2006.02.052, 2006..
- Murphy, S., Agrawal, H., Sorooshian, A., Padró, L. T., Gates, H., Hersey, S., Welch, W. A., Jung, H., Miller, J. W., Cocker III, D. R., Nenes, A., Jonsson, H. H., Flagan, R. C., and Seinfeld, J. H.: Comprehensive simultaneous shipboard and airborne characterization of exhaust from a modern container ship at sea, *Environ. Sci. Technol.*, 43, 4626–4640, 2009.
- Olmez, I. and Gordon, G. E.: Rare earths: Atmospheric signatures for oil-fired power plants and refineries, *Science*, 6, 966–968, 1985.
- Pandolfi, M., Gonzalez-Castanedo, Y., Alastuey, A., d. I. Rosa, J., Mantilla, E., d. I. Campa, A. S., Querol, X., Pey, J., Amato, F., and Moreno, T.: Source apportionment of PM₁₀ and PM_{2.5} at multiple sites in the strait of Gibraltar by PMF: impact of shipping emissions, *Environ. Sci. Pollut. Res.*, 18, 260–269, 2011.
- Schembari, C., Bove, M. C., Cuccia, E., Cavalli, F., Hjorth, J., Massabò, D., Nava, S., Udusti, R., and Prati, P.: Source apportionment of PM₁₀ in the Western Mediterranean based on observations from a cruise ship, *Atmos. Environ.*, 98, 510–518, 2014.
- Sellitto, P., Zanetel, C., di Sarra, A., Salerno, G., Tapparo, A., Meloni, D., Pace, G., Caltabiano, T., Briole, P., and Legras, B.: The impact of Mount Etna sulfur emissions on the atmospheric composition and aerosol properties in the central Mediterranean: a statistical analysis over the period 2000–2013 based on observations and Lagrangian modelling, *Atmos. Environ.*, 148, 77–88, 2017.
- Shah, S. D., Cocker, D. R., Miller, J. W., and Norbeck, J. M.: Emission rates of particulate matter and elemental and organic carbon from in-use diesel engines, *Environ. Sci. Technol.*, 38, 2544–2550, 2004.
- Simo, R., Colom-Altes, M., Grimalt, J. O., and Albaiges, J.: Background levels of atmospheric hydrocarbons, sulphate and nitrate over the Western Mediterranean, *Atmos. Environ.*, 29, 1487–1500, 1991.
- Sippula, O., Hokkinen, J., Puustinen, H., Yli-Pirilä, P., and Jokiniemi, J.: Comparison of particle emissions from small heavy fuel oil and wood-fired boilers, *Atmos. Environ.*, 43, 4855–4864, 2009.
- Sippula, O., Stengel, B., Sklorz, M., Streibel, T., Rabe, R., Orasche, J., Lintelmann, J., Michalke, B., Abbaszade, G., Radischat, C., Gröger, T., Schnelle-Kreis, J., Harndorf, H., and Zimmermann, R.: Particle emissions from a marine engine: chemical composition and aromatic emission profiles under various operating conditions, *Environ. Sci. Technol.*, 48, 11721–11729, 2014.
- Skamarock, W. C., Klemp, J. B., Dudhia, J., Gill, D. O., Barker, D. M., Huang, X. Z., Wang, W., and Powers, J. G.: A Description of the Advanced Research WRF Version 3, Technical report, Mesoscale and Microscale Meteorology Division, NCAR, Boulder, Colorado, 2008.
- Solomos, S., Amiridis, V., Zanis, P., Gerasopoulos, E., Sofiou, F. I., Herekakis, T., Brioude, J., Stohl, A., Kahn, R. A., and Kontoes, C.: Smoke dispersion modeling over complex terrain using high resolution meteorological data and satellite observations – The FireHub platform, *Atmos. Environ.*, 119, 348–361, 2015.
- Stein, A. F., Draxler, R. R., Rolph, G. D., Stunder, B. J. B., Cohen, M. D., and Ngan, F.: NOAA's HYSPLIT atmospheric transport and dispersion modeling system, *B. Am. Meteorol. Soc.*, 96, 2059–2077, doi:10.1175/BAMS-D-14-00110.1, 2015.
- Stern, N.: *The Economics of Climate Change: The Stern Review*, Cambridge University Press, Cambridge, New York, 2007.
- Trozzi, C., Vaccaro, R., and Nicolo, L.: Air pollutants emissions estimate from maritime traffic in the Italian harbours of Venice and Piombino, *Sci. Total Environ.*, 169, 257–263, 1995.
- Tsyro, S. G.: To what extent can aerosol water explain the discrepancy between model calculated and gravimetric PM₁₀ and PM_{2.5}?, *Atmos. Chem. Phys.*, 5, 515–532, doi:10.5194/acp-5-515-2005, 2005.
- Turpin, B. J. and Lim, H. J.: Species contributions to PM_{2.5} mass concentrations: Revisiting common assumptions for estimating organic mass, *Aerosol Sci. Tech.*, 35, 602–610, 2001.

- Viana, M., Kuhlbusch, T. A. J., Querol, X., Alastuey, A., Harrison, R. M., Hopke, P. K., Winiwarter, W., Vallius, M., Szidat, S., Prévôt, A. S. H., Hueglin, C., Bloemen, H., Wählin, P., Vecchi, R., Miranda, A. I., Kasper-Giebl, A., Maenhaut, W., and Hitzenberger, R.: Source apportionment of particulate matter in Europe: a review of methods and results, *J. Aerosol Sci.*, 39, 827–849, 2008.
- Viana, M., Amato, F., Alastuey, A., Querol, X., Moreno, T., Santos, S. G. D., Herce, M. D., and Fernández-Patier, R.: Chemical tracers of particulate emissions from commercial shipping, *Environ. Sci. Technol.*, 43, 7472–7477, 2009.
- Viana, M., Hammingh, P., Colette, A., Querol, X., Degraeuwe, B., de Vlieger, I., and van Aardenne, J.: Impact of maritime transport emissions on coastal air quality in Europe, *Atmos. Environ.*, 90, 96–105, 2014.
- WHO – World Health Organization: Health Effects of Particulate Matter, Policy Implications for Countries in Eastern Europe, Caucasus and Central Asia, Regional office for Europe, Copenhagen, Denmark, 2013.
- Wu, C., Huang, X. H. H., Ng, W. M., Griffith, S. M., and Yu, J. Z.: Inter-comparison of NIOSH and IMPROVE protocols for OC and EC determination: implications for inter-protocol data conversion, *Atmos. Meas. Tech.*, 9, 4547–4560, doi:10.5194/amt-9-4547-2016, 2016.